Table 1 Details of antibodies used in this study

Antigen	Clone	Product code	Supplier	Dilution	Antigen retrieval
p53	Mouse monoclonal DO-7	N1581	Dako cytomation	1:1	Microwave
ARID1A	Mouse monoclonal	sc-32761	Santa cruz biotechnology	1:200	Microwave
PTEN	Rabbit monoclonal, 138G6	#9559	Cell signaling	1:200	Microwave
HNF-1β	Goat polyclonal	sc-7411	Santa cruz biotechnology	1:400	Microwave
Annexin4	Rabbit polyclonal	ab33009	Abcam	1:400	Microwave
WT-1	Mouse monoclonal, 6F-H2	M3561	Dako cytomation	1:25	Proteinase K, warm bath

Table 2 Clinical data of the 46 patients

Age (y)	
Median (range)	51.1±1.8 years (range 28–91 years)
Subgroup, *n* (%)	
Pure-type CCAs	35 (76.1%)
Mixed-type CCAs	11 (23.9%)
Histological pattern of mixed-type CCAs, *n* (%)	
CCAs and EAs	2 (18.2%)
CCAs and SAs	8 (72.7%)
CCAs and EAs and SAs	1 (9.1%)
FIGO stage, *n* (%)	
I	33 (71.7%)
II	4 (8.7%)
III	7 (15.2%)
IV	2 (4.3%)
Endometriosis, *n* (%), median age (y)	
with endometriosis	34 (73.9%), 49.4±1.7 years *
without endometriosis	12 (26.1%), 55.5±4.7 years *

CCAs clear cell adenocarcinomas, *EAs* endometrioid adenocarcinomas, *SAs* serous adenocarcinomas

* $P < 0.012$

divided into four categories: 0, negative; 1, weakly positive; 2, moderately positive; 3, strongly positive. The most intensely staining slides were deemed to be the upper limit. The quantity of cells stained was scored as follows: 0, no staining; 1, 1–10 %; 2, 11–50 %; 3, 51–80 %; 4 >80 % of tumor nuclei stained. With p53 staining, the multiplied immunoreactive score of 8–12 was considered strong immunoreactivity, 4–6 was moderate, 1–3 was weak, and 0 was negative. It was previously indicated that all carcinomas with strong immunoreactivity (score 8–12) showed p53 missense mutations, although some negative carcinomas (score 0) also revealed p53 frameshift mutations [25]. For ARID1A and PTEN, we defined loss of function as negative nuclear staining by the multiplied immunoreactive score, inversely with p53, because previous studies showed that negative staining of ARID1A and PTEN demonstrated gene mutation [20–24, 26, 27]. HNF-1β, Annexin 4, and WT-1 were binarized as negative or positive, and immunostaining in >50 % of tumor cells was positive [28–30].

Statistical analysis

The χ^2 test and Student's t test for unpaired data were used for statistical analysis. Patient survival distribution was calculated using the Kaplan–Meier method. The significance of the survival distribution in each group was tested by the log rank test. $P < 0.05$ was considered to be statistically significant. All values were given as the mean ± SD.

Results

Patient characteristics

The characteristics of the study population are presented in Table 2. Median age at diagnosis was 51.1 ± 1.8 years (range 28–91 years). Of the 46 tumors, 71.7 % were stage I, 8.7 % were stage II, 15.2 % were stage III, and 4.3 % were stage IV (FIGO classification). Endometriosis was histologically observed in 34/46 (73.9 %) of the cases. Patients with endometriosis were aged 49.4 ± 1.7 years, whereas those without endometriosis were aged 55.5 ± 4.7 years, showing that those with endometriosis were significantly younger ($P < 0.012$).

We identified 35 pure-type CCAs and 11 mixed-type CCAs coexisting with serous or/and endometrioid elements. Mixed-type CCAs coexisting with mucinous

Table 3 Characteristics of pure-type and mixed-type CCAs

Pure-type CCAs (total number: 35)		
FIGO stage, *n* (%)		Recurrence and/or dead, n
I	29 (82.9%)	3
II	3 (8.6%)	0
III	2 (5.7%)	1
IV	1 (2.9%)	0
Existence of endometriosis, *n* (%), median age (y)		
with endometriosis	29 (82.9%), 49.1±1.8 years	4
without endometriosis	6 (17.1%), 63.4±6.2 years **	0
Mixed-type CCAs (total number: 11)		
FIGO stage, *n* (%)		
I	4 (36.4%)	0
II	1 (9.1%)	0
III	5 (45.5%)	3
IV	1 (9.1%)	0
Existence of endometriosis, *n* (%), median age (y)		
with endometriosis	5 (45.5%), 51.0±4.2 years	2
without endometriosis	6 (54.5%), 46.3±5.4 years	1

CCAs clear cell adenocarcinomas, *EAs* endometrioid adenocarcinomas, *SAs* serous adenocarcinomas

** $P < 0.005$

adenocarcinoma were not observed in our cases. The characteristics of pure-type and mixed-type CCAs are presented in Table 3. In pure-type CCAs, patients with endometriosis were younger than those without endometriosis ($P < 0.005$). In contrast, in mixed-type CCAs, there was no correlation between age and endometriosis.

Immunohistochemical findings

In 46 cases, negative staining (score 0) of ARID1A, strong positive staining (score 8–12) of p53, and negative staining (score 0) of PTEN were observed in 28 (60.9 %), 10 (21.7 %), and 2 (4.3 %) cases, respectively.

Positive staining of Annexin 4, HNF-1β, and WT-1 was found in 38 (82.6 %), 36 (78.3 %), and 3 (6.5 %) of 46 cases.

In pure-type CCAs, the immunohistochemical results are shown in Table 4. The negative staining of ARID1A, strong positive staining of p53, and negative staining of PTEN were observed in 23 (65.7 %), 5(14.3 %) and 0 (0.0 %) of 35 cases, respectively. Positive expressions of Annexin 4, HNF-1β, and WT-1 were observed in 35 (100.0 %), 34 (97.1 %), and 0(0.0 %) 35 cases, respectively. Endometriosis was observed in 18 (78.3 %) of 23 cases with negative staining of ARID1A, and in 4 (80.0 %) of five cases with strong positive staining of p53.

The immunohistochemistry results of mixed-type CCAs are demonstrated in Figs. 1 and 2. Two cases composed of CCAs and EAs had negative staining of PTEN in both areas of the CCAs and EAs (Fig. 2a–d). Eight cases composed of CCAs and SAs had various expression patterns. Negative staining of ARID1A in areas of the CCAs

Table 4 Number of cases observed with altered expression by immunohistochemical analysis in pure-type CCAs

Total number of pure-type CCAs 35				
Markers	Altered expression, *n* (%)	Endometriosis, *n* (%) in cases of altered expression	Recurrences and/or deaths, *n* (%) in cases of altered expression	Altered expression, *n* (%) in 4 recurrence and/or dead cases
ARID1A	23 (65.7 %)	18/23 (78.3 %)	0/23 (0.0 %)	0/4 (0.0 %)
p53	5 (14.3 %)	4/5 (80.0 %)	3/5 (60.0 %)	3/4 (75.0 %)
PTEN	0 (0.0 %)	0 (0.0 %)	0 (0.0 %)	0/4 (0.0 %)
ARID1A and p53	1 (2.9 %)	0/1 (0.0 %)	0/1 (0.0 %)	0/4 (0.0 %)
Annexin4	35 (100.0 %)	29/35 (82.9 %)	4/35 (11.4 %)	4/4 (100.0 %)
HNF-1β	34 (97.1 %)	29/34 (85.3 %)	4/34 (11.8 %)	4/4 (100.0 %)
WT-1	0 (0.0 %)	0 (0.0 %)	0 (0.0 %)	0/4(0.0 %)

CCAs clear cell adenocarcinomas

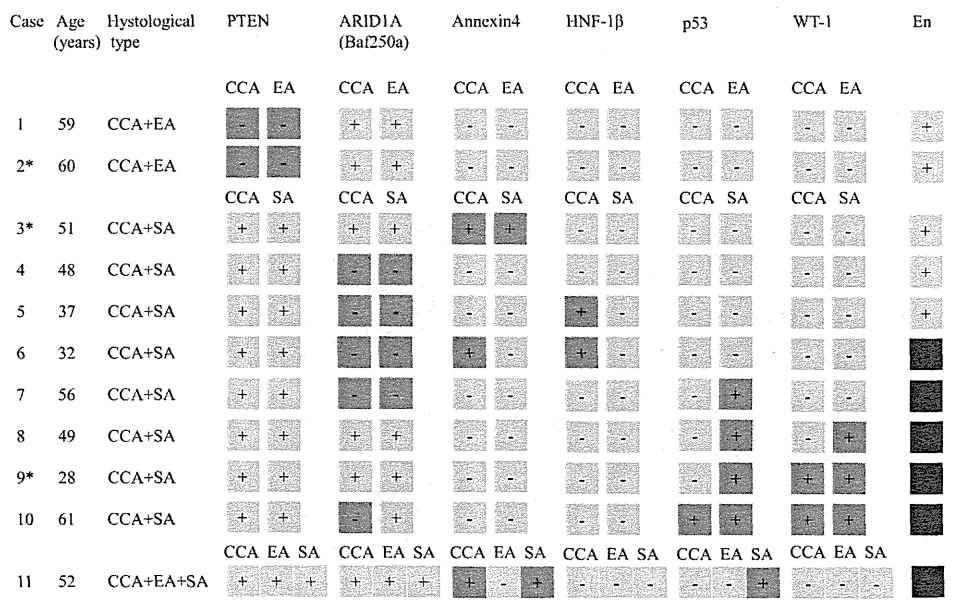

Fig. 1 Immunohistochemical characteristics in mixed-type CCAs. Positive immunostaining is demonstrated as *plus*, and negative as *minus*. Abnormal expression is surrounded by red. *EA* endometrioid adenocarcinoma, *SA* serous adenocarcinoma, respectively. *En* endometriosis; *plus* surrounded with *yellow* indicates that endometriosis was observed; *minus* surrounded with *green* indicates that endometriosis was not found. *Asterisk* recurrence and/or death

was observed in 5/8 (62.5 %), and in one case among these five cases positive staining of ARID1A was found in SAs (Fig. 2e–h). Strong positive staining of p53 in areas of the SAs was found in 4 (50.0 %) of eight cases, and in one case among of these four cases positive staining was observed in both areas of the CCAs and SAs (Fig. 2i–l). The negative staining of PTEN was not observed in all eight cases. One case composed of CCA, EA, and SA had altered expression of Annexin 4 and p53 without endometriosis.

Overall, in pure-type CCAs, the frequency of endometriosis was high. There was no significant difference between the involvement of endometriosis and expression of each protein. However, in mixed-type CCAs, endometriosis was not found in any of the p53 strong positive staining cases.

Patient prognosis

Of 35 patients with pure-type CCAs, 29 (82.9 %) had stage I disease, 3 (8.5 %) had stage II, 2 (5.7 %) had stage III, and 1 (2.9 %) had stage IV. In pure-type CCAs, the median survival time was 65.5 months (range 31–194 months), and recurrence and/or death occurred in 4/35 (11.4 %). In these 4 cases, negative staining of ARID1A was not found; however, strong positive staining of p53 was observed 3/4 (75.0 %) (Table 4). This indicated that altered expression of ARID1A and p53 showed contrary prognosis ($P < 0.001$).

Of 11 patients with mixed-type CCAs, 4 (36.4 %) had stage I disease, 1 (9.1 %) had stage II, 5 (45.4 %) had stage III, and 1 (9.1 %) had stage IV. In mixed-type CCAs, the median survival time was 60.4 months (range 1–160 months) and recurrence and/or death occurred in 3/11 (27.3 %). In patients with recurrence and/or death, a significant difference between prognosis and expression of p53 and ARID1A was not found.

Discussion

Recent pathological and molecular evidences have suggested that endometriosis serves as a precursor of CCAs [21, 31, 32]. In approximately 60 % of endometriosis-associated EOAs including CCAs, the carcinomas are adjacent to endometriosis or arise directly from atypical endometriosis, suggesting that malignant transformation

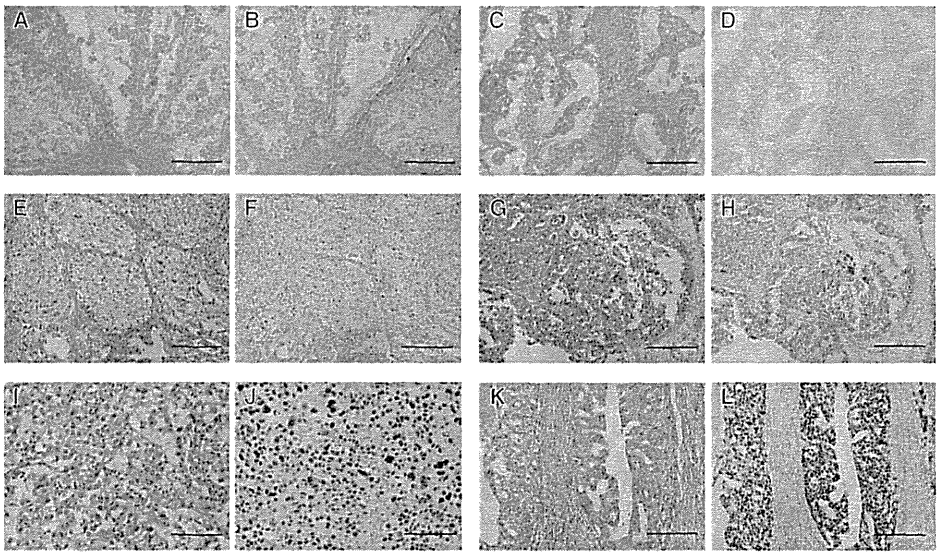

Fig. 2 Immunohistochemistry of mixed-type CCAs. **a–d** Case 1 of Fig. 2 is presented. **a**, **b** In the area of CCAs, PTEN was negative in the nucleus or cytoplasm of glandular cells. **c**, **d** In the area of EAs, PTEN was negative in the nucleus or cytoplasm of glandular cells. **e–l** Case 10 of Fig. 2 is presented. **e**, **f** In the area of CCAs, ARID1A was negative in the nucleus of glandular cells. **g**, **h** In the area of SAs, ARID1A was positive in the nucleus of glandular cells. **i**, **j** In the area of CCAs, p53 was positive in the nucleus of glandular cells. **k**, **l** In the area of SAs, p53 was positive in the nucleus of glandular cells. **a–l** ×100. *Scale bar* 200 μm

occurs in a subset of patients with ovarian endometriosis. In our current study, endometriosis was also histopathologically observed in 73.9 % of CCAs. Among pure-type CCAs selected in this study, endometriosis was observed in 82.9 % of cases, and patients with endometriosis were significantly younger than those without endometriosis. These results show that endometriosis represents an important site of the origin of pure-type CCAs. However, endometriosis was observed in 45.5 % of mixed-type CCAs, and there was no significant difference between the ages of patients with and without endometriosis. Furthermore, as for the prognosis, the ratio of cases of recurrences and/or deaths of mixed-type CCAs was higher than pure-type CCAs. This demonstrated that difference of characteristic between pure-type and mixed-type CCAs.

The p53 gene is the most frequently altered gene in human cancer [25]. Recently, it was reported that mutation of p53 was an important determinant of aggressive biological behavior, resulting in poor outcome of patients with several types of cancer [33]. In contrast, changes in chromatin can influence the epigenetic regulation of many genes, inducing transcription, DNA replication, and DNA damage repair in cancer. Chromatin remodeling is essential for all nuclear activities, and ARID1A is a chromatin remodeling factor [24, 25]. ARID1A is recognized as a tumor suppressor gene and also provides a potential approach to determine which of the numerous epigenetic changes in cancer confer a selective growth advantage. It was previously reported that the AIRD1A mutation is an early event in neoplastic transformation as well as p53 [22, 23, 34]. Importantly, the regulation of p53-related genes by ARID1A raises the possibility that ARID1A molecularly cooperates with p53 to inhibit tumor growth. Therefore, it is possible that in non-transformed cells, ARID1A and p53 collaborate as a pair of gatekeepers that prevent carcinogenesis by transcriptional activation of tumor-inhibiting downstream genes. Furthermore, it is thought that concurrent mutations in ARID1A and p53 are not required for carcinogenesis; in other words, both genes are mutually exclusive in tumor [22].

With the exception of one case, our immunohistochemical analysis demonstrated that in pure-type CCAs, tumors with mutated ARID1A contain wild-type p53 and tumors with mutated p53 harbor wild-type ARID1A. Both ARID1A and p53 appear to be essential for tumor suppression of pure-type CCAs, and concurrent mutations in

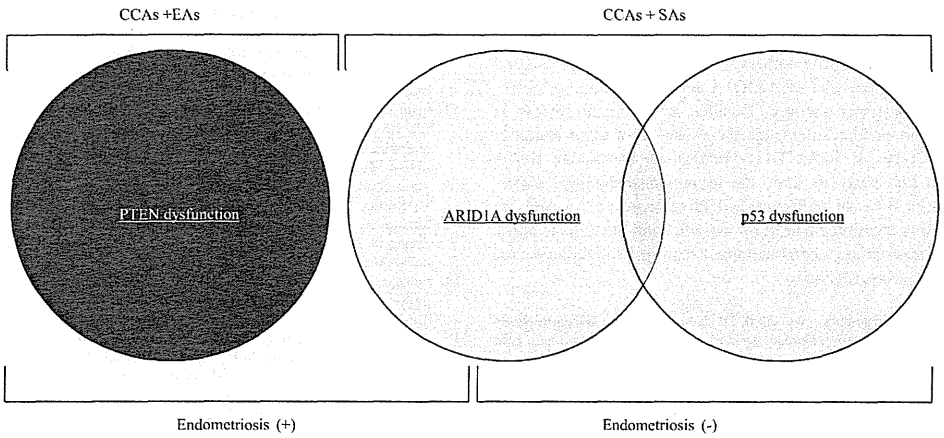

Fig. 3 Association between dysfunction of tumor suppressor genes and endometriosis in mixed-type CCAs. This figure presents a concise summary of mixed-type CCAs with altered expression of PTEN, p53, and/or ARID1A. Mixed-type CCAs lacking PTEN and ARID1A function were associated with endometriosis. Mixed-type CCAs lacking p53 function were not associated with endometriosis

both genes are not required for their carcinogenesis. Our results also suggest that ARID1A and p53 genes were mutually exclusive in CCAs [22]. Interestingly, we found altered expression of p53 and normal expression of ARID1A in pure-type CCAs with recurrence or death. Conversely, we found altered expression of ARID1A and normal expression of p53 in pure-type with good prognosis. This result indicated that pure-type CCAs may be divided into two subgroups with mutation in either ARID1A or p53; these subgroups correlate with prognosis. Henceforward, recognition of this subgroup of CCAs may play an indispensable role in determining patient prognosis and selecting the appropriate chemotherapy.

In this study, 11 cases were categorized by the present pathological review into mixed-type CCAs. Immunohistochemical results indicated that mixed-type CCAs could be divided into at least four groups accompanied with dysfunction of tumor suppressor genes, PTEN, ARID1A and/or p53, correlated with endometriosis: (1) In mixed-type CCAs coexisting with EAs lacking PTEN function, endometriosis was observed. This type of CCAs may have the characteristics of EAs, indicating intratumoral heterogeneity of CCAs. (2) In mixed-type CCAs coexisting with SAs lacking ARID1A function, endometriosis was observed. Altered expression of Annexin 4 or HNF-1β was found. These characteristics of CCAs were observed in the area of SAs, indicating intratumoral heterogeneity. (3) In mixed-type CCAs coexisting with SAs lacking p53 function, endometriosis was not observed. In these CCAs, ARID1A function was preserved. Altered expression of WT-1 was found in the area of CCAs. These results implied the intratumoral heterogeneity of CCAs showing the characteristics of SAs. (4) In mixed-type CCAs coexisting with SAs lacking both ARID1A and p53 function, endometriosis was not observed. These findings indicated intratumoral heterogeneity of CCAs that exhibited the characteristics of both CCAs and SAs (Fig. 3). These immunohistochemical results demonstrated that mixed-type CCAs containing SAs with altered expression of p53 exhibited different carcinogenesis from other mixed-type CCAs, independent of endometriosis. Furthermore, the rates of altered expression of Annexin 4 and HNF-1β were lower, and expression of WT-1 was higher than in pure-type CCAs. These immunostaining results also led us to infer that mixed-type CCAs have different characteristics from pure-type CCAs.

Conclusion

We revealed that CCAs should be first divided into two subgroups: pure type and mixed type. Furthermore, in clinical practice, we must consider that it is necessary to examine the molecular characteristics of individual CCAs. CCAs must be categorized into three subtypes: pure-type CCAs, CCAs with serous characteristics, and CCAs with other histological characteristics. We must deal with CCAs according to intratumoral heterogeneity, and these findings may be applied to clinical treatment, including chemotherapy. Moreover, we should consider intratumoral

heterogeneity because the difference in expression between ARID1A and p53 can influence the prognosis in pure-type CCAs. A new chemotherapy strategy is necessary, based on the expression of ARID1A and p53, including molecular targeting therapy. Detailed pathological review is important to acknowledge the existence of other histological types of EOAs. To the best of our knowledge, this is the first study to show the immunohistochemical differences between pure-type and mixed-type CCAs, and the first to mention the need for classification of CCAs to apply to appropriate chemotherapy according to clinicopathological heterogeneity.

Acknowledgments We thank Dr. Ken-ichi Iyama (Department of Surgical Pathology, Kumamoto University Hospital) for his help with the diagnosis of the 46 cases. We also thank Ms. Ai Aoki (Department of Obstetrics and Gynecology, Faculty of Life Sciences, Kumamoto University) for her technical assistance. This research was supported by a grant from Grants-in-Aid for Scientific Research (B) 21390454.

Conflict of interest The authors have no conflict of interest.

References

1. Peham H (1899) Aus accessorischen nebennieren-anlage entstandene ovarial-tumore. Monatschr Geburtsch Gynäk 10:685–687
2. Schiller W (1939) Mesonephroma ovarii. Am J Cancer 35:1–21
3. Scully RE, Barlow JF (1967) "Mesonephroma" of the ovary: tumor of Müllerian nature related to endometrioid carcinoma. Cancer 20:1405–1412
4. Serov SF, Scully RE, Jobin LH (1973) Histologic typing of ovarian tumors. In: Scully RE ed World Health Organization. International Histological Classification of Tumours. Geneva: Springer. p37–42
5. Sugiyama T, Kamura T, Kigawa J, Terakawa N, Kikuchi Y, Kita T, Suzuki M, Sato I, Taguchi K (2000) Clinical characteristics of clear cell carcinoma of the Ovary. Cancer 11:2584–2589
6. del Carmen MG, Birrer M, Schorge JO (2012) Clear cell carcinoma of the ovary: a review of the literature. Gynecol Oncol 126:481–490
7. Takano M, Kikuchi Y, Yaegashi N, Kuzuya K, Ueki M, Tsuda H, Kigawa J, Takeuchi S, Tsuda H, Moriya T, Sugiyama T (2006) Clear cell carcinoma of the ovary: a retrospective multicentre experience of 254 patients with complete surgical staging. Br J Cancer 94:1369–1374
8. Pectasides D, Fountzilas G, Aravantinos G, Kalofonos C, Efstathiou H, Farmakis D, Skarlos D, Pavlidis N, Economopoulos T, Dimopoulos MA (2006) Advanced stage clear-cell ovarian cancer: the Hellenic cooperative oncology group experience. Gynecol Oncol 102:285–291
9. Ho CM, Huang YJ, Chen TC, Huang SH, Liu FS, Chang Chien CC, Yu MH, Mao TL, Wang TY, Hsieh CY (2004) Pure-type clear cell carcinoma of the ovary as a distinct histologic type and improved survival in patients treated with paclitaxel-platinum-based chemotherapy in pure-type advanced disease. Gynecol Oncol 94:197–203
10. Utsunomiya H, Akahira J, Tanno S, Moriya T, Toyoshima M, Niikura H, Ito K, Morimura Y, Watanabe Y, Yaegashi N (2006) Paclitaxel-platinum combination chemotherapy for advanced or recurrent ovarian clear cell adenocarcinoma: a multicenter trial. Int J Gynecol Cancer 16:52–56
11. Recio FO, Piver MS, Hempling RE, Driscol DL (1996) Lack of improved survival plus increase in thromboembolic complications in patients with clear cell carcinoma of the ovary treated with platinum versus nonplatinum-based chemotherapy. Cancer 78:2157–2163
12. Rauh-Hain JA, Winograd D, Growdon WB, Goodman AK, Boruta DM 2nd, Schorge JO, del Carmen MG (2012) Prognostic determinants in patients with uterine and ovarian clear cell carcinoma. Gynecol Oncol 125:376–380
13. Veras E, Mao TL, Ayhan A, Ueda S, Lai H, Hayran M, Shih Ie M, Kurman RJ (2009) Cystic and adenofibromatous clear cell carcinomas of the ovary: distinctive tumors that differ in their pathogenesis and behavior: a clinicopathologic analysis of 122 cases. Am J Pathol 33:844–853
14. Kurman RJ, Shih Ie M (2010) The origin and pathogenesis of epithelial ovarian cancer: a proposed unifying theory. Am J Pathol 34:433–443
15. Yamamoto S, Tsuda H, Shimazaki H, Takano M, Yoshikawa T, Kuzuya K, Tsuda H, Kurachi H, Kigawa J, Kikuchi Y, Sugiyama T, Matsubara O (2011) Clear cell adenocarcinoma with a component of poorly differentiated histology: a poor prognostic subgroup of ovarian clear cell adenocarcinoma. Int J Gynecol Pathol 30:431–441
16. Veras E, Mao TL, Ayhan A, Ueda S, Lai H, Hayran M, Shih Ie M, Kurman RJ (2009) Cystic and adenofibromatous clear cell carcinomas of the ovary: distinctive tumors that differ in their pathogenesis and behavior: a clinicopathologic analysis of 122 cases. Am J Surg Pathol 33:844–853
17. Kurman RJ, Craig JM (1972) Endometrioid and clear cell carcinoma of the ovary. Cancer 29:1653–1664
18. Han G, Gilks CH, Leung S, Ewanowich CA, Irving JA, Longacre TA, Soslow RA (2008) Mixed ovarian epithelial carcinomas with clear cell and serous components are variants of high-grade serous carcinoma: an interobserver correlative and immunohistochemical study of 32 cases. Am J Surg Pathol 32:955–964
19. Köbel M, Kalloger SE, Huntsman DG, Santos JL, Swenerton KD, Seidman JD, Gilks CB, Cheryl Brown Ovarian Cancer Outcomes Unit of the British Columbia Cancer Agency, Vancouver BC (2010) Differences in tumor type in low-stage versus high-stage ovarian carcinomas. Int J Gynecol Pathol 29:203–211
20. Jones S, Wang TL, Shih Ie M, Mao TL, Nakayama K, Roden R, Glas R, Slamon D, Diaz LA Jr, Vogelstein B, Kinzler KW, Velculescu VE, Papadopoulos N (2010) Frequent mutations of chromatin remodeling gene ARID1A in ovarian clear cell carcinoma. Science 8:228–231
21. Wiegand KC, Shah SP, Al-Agha OM, Zhao Y, Tse K, Zeng T, Senz J, McConechy MK, Anglesio, Kalloger SE, Yang W, Heravi-Moussavi A, Giuliany R, Chow C, Fee J, Zayed A, Prentice L, Melnyk N, Turashvili G, Delaney AD, Madore J, Yip S, McPherson AW, Ha G, Bell L, Fereday S, Tam A, Galletta L, Tonin PN, Provencher D, Miller D, Jones SJ, Moore RA, Morin GB, Oloumi A, Boyd N, Aparicio SA, Shih Ie M, Mes-Masson AM, Bowtell DD, Hirst M, Gilks B, Marra MA, Huntsman DG (2010) ARID1A mutations in endometriosis-associated ovarian carcinoma. N Engl J Med 363:1532–1543
22. Guan B, Wang TL, Shih Ie M (2011) ARID1A, a factor that promotes formation of SWI/SNF-mediated chromatin remodeling, is a tumor suppressor in gynecologic cancers. Cancer Res 71:6718–6727
23. Guan B, Gao M, Wu CH, Wang TL, Shih Ie M (2012) Functional analysis of in-frame indel ARID1A mutations reveals new regulatory mechanisms of its tumor suppressor functions. Neoplasia 14:986–993
24. Wu CH, Mao TL, Vang R, Ayhan A, Wang TL, Kurman RJ, Shie Ie M (2012) Endocervical-type mucinous borderline tumors are

related to endometrioid tumors based on mutation and loss of expression of ARID1A. Int J Gynecol Pathol 31:297–303
25. Tashiro H, Isacson C, Levine R, Kurman RJ, Cho KR, Hedrick L (1997) p53 gene mutations are common in uterine serous carcinoma and occur early in their pathogenesis. Am J Pathol 150:177–185
26. Sato N, Tsunoda H, Nishida H, Morishita Y, Takimoto Y, Kubo T, Noguchi M (2000) Loss of heterozygosity on 10q23.3 and mutation of the tumor suppressor gene PTEN in benign endometrial cyst of the ovary: possible sequence progression from benign endometrial cyst to endometrioid carcinoma and clear cell carcinoma of the ovary. Cancer Res 60:7052–7056
27. An HJ, Lee NH, Shim JY, Kim JY, Lee C, Kim SJ (2002) Alteration of PTEN expression in endometrial carcinoma is associated with down-regulation of cyclin-dependent kinase inhibitor, p27. Histopathology 41:437–445
28. Miao Y, Cai B, Liu L, Yang Y, Wan X (2009) Annexin 4 is differentially expressed in clear cell carcinoma of the ovary. Int J Gynecol Cancer 19:1545–1549
29. Kajihara H, Yamada Y, Kanayama S, Furukawa N, Noguchi T, Haruta S, Yoshida S, Sado T, Oi H, Kobayashi H (2010) Clear cell carcinoma of the ovary: potential pathologic mechanisms (Review). Oncol Rep 23:1193–1203
30. Köbel M, Turbin D, Kalloger SE, Gao D, Huntsman DG, Gilks CB (2011) Biomarker expression in pelvic high-grade serous carcinoma: comparison of ovarian and omental sites. Int J Gynecol Pathol 30:366–371
31. DeLair D, Oliva E, Köbel M, Macias A, Gilks CB, Soslow RA (2011) Morphologic spectrum of immunohistochemically characterized clear cell carcinoma of the ovary: a study of 155 cases. Am J Pathol 35:36–44
32. Jiang X, Morland SJ, Hitchcock A, Thomas EJ, Campbell IG (1998) Allelotyping of endometriosis with adjacent ovarian carcinoma reveals evidence of a common lineage. Cancer Res 58:1707–1712
33. Ichikawa A, Kinoshita T, Watanabe T, Kato H, Nagai H, Tsushita K, Saito H, Hotta T (1997) Mutations of the p53 gene as a prognostic factor in aggressive B-cell lymphoma. N Engle J Med 337:529–534
34. Ayhan A, Mao TL, Seckin T, Wu Ch, Guan B, Ogawa H, Futagami M, Mizukami H, Yokoyama Y, Kurman RJ, Shih Ie M (2012) Loss of ARID1A expression is an early molecular event in tumor progression from ovarian endometriotic cyst to clear cell and endometrioid carcinoma. Int J Gynecol Cancer 22:1310–1315

THE JOURNAL OF
Obstetrics and Gynaecology Research

doi:10.1111/jog.12561 J. Obstet. Gynaecol. Res. Vol. 41, No. 4: 623–627, April 2015

Embolization for post-partum rupture of ovarian artery aneurysm: Case report and review

Isao Sakaguchi[1], Takashi Ohba[1], Osamu Ikeda[2], Yasuyuki Yamashita[2] and Hidetaka Katabuchi[1]

Departments of [1]Obstetrics and Gynecology and [2]Diagnostic Radiology, Faculty of Life Sciences, Kumamoto University, Kumamoto, Japan

Abstract

Spontaneous rupture of an ovarian artery aneurysm most commonly presents with abdominal pain in a multiparous woman in the early post-partum period. Aneurysms of the ovarian artery have been reported in the published work very infrequently. In our case, a 31-year-old multiparous woman experienced sudden left lower quadrant abdominal pain on the second post-partum day. Angiography showed rupture of a left ovarian artery aneurysm, which was successfully embolized using gelatin sponge particles. The patient resumed menstruation 3 months after the embolization and concurrently conceived, ultimately giving birth at term without complications. Interventional radiology appears to be a highly safe and effective technique for diagnosis and management of a ruptured ovarian artery aneurysm with minimal risk of impairing subsequent fertility.

Key words: angiography, early post-partum period, fertility, ovarian artery aneurysm, transcatheter arterial embolization.

Introduction

Spontaneous rupture of an ovarian artery aneurysm is extremely rare; 21 cases have been reported in the English-language published work during the past 5 decades. The episodes tend to occur during pregnancy or in the early post-partum period. Here we report a case of spontaneous rupture of the left ovarian artery in the early post-partum period and also review the published reports about this condition. Written consent was obtained from the patient.

Case

A 31-year-old woman, gravida 6, para 4, with a history of cesarean delivery 13 years ago, was transferred to our University Hospital complaining of severe lower abdominal pain 2 days after a vaginal delivery at 39 weeks of gestation. Her pregnancy course had been uneventful. In late pregnancy, her blood count showed a white blood cell count of 11 700/mm^3, hemoglobin 10.7 g/dL, and platelets 270 000/mm^3. She gave birth to a healthy male infant weighing 2958 g in a local clinic, and the placenta was delivered spontaneously. Examination following delivery revealed a minimal tear of the cervix, which was repaired properly. The estimated blood loss was 378 g.

On the second post-partum day, the patient experienced sudden onset of abdominal pain in the left lower quadrant, and she was immediately transferred to our hospital by ambulance. On arrival, she was alert but appeared uncomfortable due to the pain. At the initial physical examination, her vital signs indicated body temperature, 37.1°C; heart rate, 92 b.p.m.; respiratory rate, 16 breaths/min; and blood pressure, 96/56 mmHg. Abdominal examination showed left

Received: April 28 2014.
Accepted: August 5 2014.
Reprint request to: Dr Isao Sakaguchi, Department of Obstetrics and Gynecology, Faculty of Life Sciences, Kumamoto University, Honjo 1-1-1, Chuo-Ku, Kumamoto-City, Kumamoto 860-8556, Japan. Email: isakakuh@gmail.com

lower quadrant tenderness without rebound. Initial laboratory test results indicated an elevated white blood cell count of 16 700/mm^3 and a decreased hemoglobin level of 7.9 g/dL. Ultrasonographic examination of the abdomen and pelvis demonstrated no intraperitoneal effusion, but an 8-cm-diameter hematoma was visualized inferior to the left kidney. Enhanced computed tomography (CT) of the abdomen and pelvis confirmed a massive hematoma inferior to the left kidney that extended to the left retroperitoneal region (Fig. 1). Tortuous vascular structures were observed beside the hematoma and there was no extravasation.

A reformatted CT scan indicated that the tortuous vessel was the left ovarian artery with an aneurysm formation (Fig. 2). There was no indication of rupture or dehiscence of the uterine scar from the previous cesarean delivery on magnetic resonance imaging (MRI) or ultrasonography, and there were no foci of actual bleeding. Therefore, we selected expectant management.

Six days after delivery, the patient's hemoglobin level decreased to 6.4 g/dL, and she received a blood transfusion. Emergent angiography was undertaken to locate the origin of bleeding. She underwent catheterization through a right femoral approach with 4-Fr catheters (Pig-tail, MIK, Duck head; Medikit) and a 2.5-Fr microcatheter (Renegerd-18; TARGET, Boston Scientific). Angiography revealed the tortuous left ovarian artery with segmental dilatations, suggesting that the ovarian artery aneurysms remained. Although there was no extravasation of the contrast medium, selective embolization of the left ovarian artery using gelatin sponge particles was performed. After embolization, an angiogram showed complete exclusion of the aneurysm, and the patient's anemia stopped progressing. Follow-up study by ultrasound examination revealed a shrinking left retroperitoneal hematoma.

The patient had an uneventful postoperative course and was discharged 14 days after the embolization. Enhanced CT 2 months after embolization demonstrated a small hematoma in the retroperitoneal space, and did not show any other aneurysm or vascular malformation. She resumed menstruation 3 months after the embolization, and she concurrently became pregnant. Twelve months after the embolization, an elective cesarean delivery was performed at 39 weeks of gestation in the local clinic. The post-partum period was uneventful.

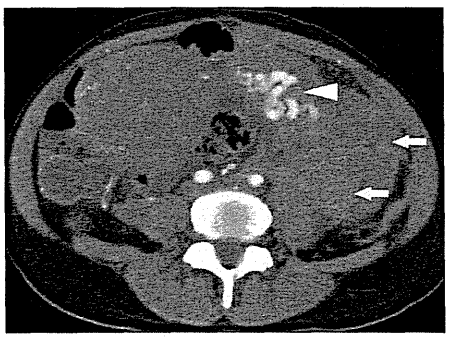

Figure 1 Abdominal computed tomography scan after injection of iodine contrast media on admission at 2 days after delivery. Transverse plane showed a large left retroperitoneal hematoma (arrows). Tortuous vascular structures on the left side of uterus (arrow head) suggested vascular aneurysm. No extravasation was found in this image.

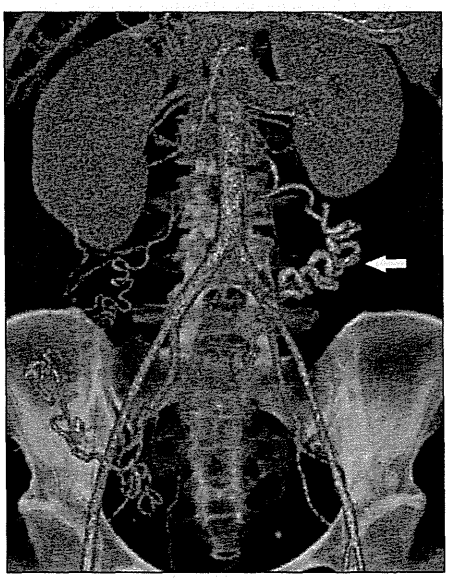

Figure 2 Reformatted computed tomography scan on admission at 2 days after delivery revealed the left torturous ovarian artery with aneurysm formation (arrow).

Discussion

The spontaneous rupture of an ovarian artery aneurysm is extremely rare. Our review of the published work revealed 21 cases of ovarian artery aneurysm dating back to 1963, as shown in Table 1.[1-21] The age of the subjects ranged from 23 to 69 years, and 14 of the 21 cases were associated with pregnancy. In 10 of those 14, the rupture of the ovarian artery aneurysm occurred within the first 5 days after delivery. In our case, the patient had sudden onset of abdominal pain 2 days after delivery, which is consistent with previous reports.

The physiology and anatomy of the cardiovascular system dramatically change during pregnancy. The enlarging uterus induces local fluctuations in blood pressure in the aorta and ovarian arteries, and dilation of the pelvic arteries occurs in conjunction with the increased uterine blood flow. It is widely accepted that involution of the uterus and the return of other genital organs to their prepregnant state in the post-partum period takes 3–4 weeks. Two mechanisms may be involved with the formation of an ovarian artery aneurysm during this time. First, failure of puerperal involution of a segment of ovarian artery after the pregnancy may induce subsequent aneurysm formation.[4] Second, there may be pregnancy-related changes in the vascular walls.[1,3,4] In a combination of animal and human studies, arterial changes were correlated with high levels of circulating steroid hormones during pregnancy.[22] Moreover, all of the 14 previously reported cases that were associated with pregnancy occurred in multiparous or grand multiparous women, just as in our case, suggesting that repeated pregnancy is a risk factor for the development of an ovarian artery aneurysm.

In the present case, the ovarian artery aneurysm during the post-partum period occurred on the left side. However, it is notable that in previous reports, 11 of the 14 cases of aneurysm associated with pregnancy were located in the right ovarian artery. Although the cause of ovarian artery aneurysms during the post-partum period remains poorly understood, there may be a connection to the physiological rotation of the gravid uterus. Post-partum uterine involution induces a dextrorotated uterus to return to the normal prepregnant position, and the associated physiological changes may be involved in the formation of ovarian artery aneurysms on the right side.

The rupture of an ovarian artery aneurysm should be considered in cases of flank pain or abdominal pain in the early post-partum period, and the diagnosis can be confirmed by a reformatted CT scan. Selective angiography is a useful tool both to identify the bleeding from the aneurysm and to manage the bleeding via transcatheter arterial embolization (TAE). In eight of the 21 cases, TAE of ovarian arteries was performed, as shown in Table 1. In two of those eight, the emergent laparotomy was performed following TAE and the ovarian artery was ligated, because embolization was unsuccessful. In our case, the patient was discharged 14 days after TAE with an uneventful recovery. Over the past 3 decades, the role of TAE has evolved from a novel treatment to a major option in the management of obstetric hemorrhage.[23] Interventional radiology has modified this attitude further by offering a minimally invasive alternative of controlling active hemorrhage.

The impact of TAE on fecundity has not been studied in great detail. Several studies have reported cases with uneventful pregnancy outcomes,[24-29] and the fertility of patients who underwent embolization of uterine arteries does not appear to be statistically different from that of the general population.[30] In our case, the patient conceived 3 months after the embolization, and uneventfully gave birth at term. There are no studies evaluating the effect of ovarian artery embolization on ovarian function. However, a follow-up study of nontarget ovarian artery embolization following uterine artery embolization suggests that most patients do not develop ovarian failure.[31] To the best of our knowledge, the present case is the first report of a successful pregnancy following unilateral ovarian artery embolization of a ruptured ovarian artery aneurysm. Larger prospective studies are required to understand fecundity following unilateral or bilateral ovarian artery embolization.

In conclusion, the rupture of an ovarian artery aneurysm should be suspected in a multiparous patient presenting with flank pain or abdominal pain in the early post-partum period. Interventional radiology is an effective technique for both diagnosis and management of a ruptured ovarian artery aneurysm, and it may be the best option for patients who wish to preserve their fecundity.

Acknowledgments

The authors thank medical colleagues in the Kumamoto University Hospital.

Disclosure

The authors have no conflicts of interest related to this article.

Table 1 Reported cases of ruptured ovarian artery aneurysm

	Reference	Year	Age (years)	Obstetric status	Onset day of pregnancy-related case	Side	Treatment	Treatment outcome
1	Caillouette and Owen[1]	1963	29	4G4P	Post-partum day 2	Left	Laparotomy	Success
2	Tsoutsoplides[2]	1967	35	6G3P	Post-partum day 4	Left	Laparotomy	Success
3	Riley[3]	1975	38	6G6P	During delivery	Right	Laparotomy	Success
4	Burnett and Carfrae[4]	1976	32	2G2P	Post-partum day 4	Right	Laparotomy	Success
5	Jafari and Saleh[5]	1977	26	5G4P	Post-partum day 1	Right	Laparotomy	Success
6	Mojab and Rodriguez[6]	1977	23	—	Post-partum month 1	Right	Laparotomy	Success
7	Siu *et al.*[7]	1986	45	6G5P	—	Left	Laparotomy	Success
8	Høgdall *et al.*[8]	1989	31	4G3P	39w of gestation	Right	Laparotomy	Success
9	King[9]	1990	36	5G5P	Post-partum day 4	Right	Embolization	Success
10	Belfort *et al.*[10]	1993	38	3G2P	Post-partum day 0	Right	Laparotomy	Success
11	Guillem *et al.*[11]	1999	38	3G2P	Post-partum day 4	Right	Embolization	Success
12	Blachar *et al.*[12]	2000	38	12G11P	Post-partum day 3	Right	Laparotomy	Success
13	Panoskaltsis *et al.*[13]	2000	37	4P	39w of gestation	Left	Laparotomy	Success
14	Manabe *et al.*[14]	2002	53	—	—	Left	Laparotomy	Success
15	Nakajo *et al.*[15]	2005	55	2G2P	—	Right	Embolization	Success
16	Kale *et al.*[16]	2005	30	5G5P	—	Left	Laparotomy	Success
17	Rathod *et al.*[17]	2005	40	—	Post-partum day 0	Right	Embolization	Success
18	Poilblanc *et al.*[18]	2008	39	5G4P	Post-partum day 5	Right	Embolization	Success
19	Kirk *et al.*[19]	2009	69	3G3P	—	Left	Embolization	Success
20	Tsai and Lien[20]	2009	48	2G2P	—	Left	Embolization and laparotomy	Embolization was unsuccessful
21	Chao and Chen[21]	2009	46	3G2P	—	Left	Embolization and laparotomy	Embolization was unsuccessful
22	Our case	2014	31	6G4P	Post-partum day 2	Left	Embolization	Success

References

1. Caillouette JC, Owen HW. Postpartum spontaneous rupture of an ovarian-artery aneurysm. *Obstet Gynecol* 1963; **21**: 510–511.
2. Tsoutsoplides GC. Post-partum spontaneous rupture of a branch of the ovarian artery. *Scott Med J* 1967; **12**: 289–290.
3. Riley PM. Rupture of right ovarian artery aneurysm during delivery. *S Afr Med J* 1975; **49**: 729.
4. Burnett RA, Carfrae DC. Spontaneous rupture of ovarian artery aneurysm in the puerperium. Two case reports and a review of the literature. *Br J Obstet Gynaecol* 1976; **83**: 744–750.
5. Jafari K, Saleh I. Postpartum spontaneous rupture of ovarian artery aneurysm. *Obstet Gynecol* 1977; **49**: 493–495.
6. Mojab K, Rodriguez J. Postpartum ovarian artery rupture with retroperitoneal hemorrhage. *AJR Am J Roentgenol* 1977; **128**: 695–696.
7. Siu KF, Luk SL, Kung TM. Spontaneous rupture of the ovarian artery. *J R Coll Surg Edinb* 1986; **31**: 237–240.
8. Høgdall CK, Pedersen SJ, Ovlisen BO, Helgestrand UJ. Spontaneous rupture of an ovarian-artery aneurysm in the third trimester of pregnancy. *Acta Obstet Gynecol Scand* 1989; **68**: 651–652.
9. King WL. Ruptured ovarian artery aneurysm: A case report. *J Vasc Surg* 1990; **12**: 190–193.
10. Belfort MA, Simon T, Kirshon B, Howell JF. Ruptured ovarian artery aneurysm complicating term vaginal delivery. *South Med J* 1993; **86**: 1073–1074.
11. Guillem P, Bondue X, Chambon JP, Lemaitre L, Bounoua F. Spontaneous retroperitoneal hematoma from rupture of an aneurysm of the ovarian artery following delivery. *Ann Vasc Surg* 1999; **13**: 445–448.
12. Blachar A, Bloom AI, Golan G, Venturero M, Bar-Ziv J. Case reports. Spiral CT imaging of a ruptured post-partum ovarian artery aneurysm. *Clin Radiol* 2000; **55**: 718–720.
13. Panoskaltsis T, Padwick M, Thomas JM, el Sayed T. Spontaneous rupture of ovarian arterial aneurysm in the antenatal period. *Acta Obstet Gynecol Scand* 2000; **79**: 718–719.
14. Manabe Y, Yoshioka K, Yanada J. Spontaneous rupture of a dissection of the left ovarian artery. *J Med Invest* 2002; **49**: 182–185.
15. Nakajo M, Ohkubo K, Fukukura Y, Nandate T, Nakajo M. Embolization of spontaneous rupture of an aneurysm of the ovarian artery supplying the uterus with fibroids. *Acta Radiol* 2005; **46**: 887–890.
16. Kale A, Akdeniz N, Erdemoglu M, Ozcan Y, Yalinkaya A. Spontaneous rupture of the ovarian artery following spontaneous vaginal birth. *Saudi Med J* 2005; **26**: 1826–1827.
17. Rathod KR, Deshmukh HL, Asrani A, Salvi VS, Prabhu S. Successful embolization of an ovarian artery pseudoaneurysm complicating obstetric hysterectomy. *Cardiovasc Intervent Radiol* 2005; **28**: 113–116.
18. Poilblanc M, Winer N, Bouvier A *et al.* Rupture of an aneurysm of the ovarian artery following delivery and endovascular treatment. *Am J Obstet Gynecol* 2008; **199**: e7–e8.
19. Kirk JS, Deitch JS, Robinson HR, Haveson SP. Staged endovascular treatment of bilateral ruptured and intact ovarian artery aneurysms in a postmenopausal woman. *J Vasc Surg* 2009; **49**: 208–210.
20. Tsai MT, Lien WC. Spontaneous rupture of an ovarian artery aneurysm. *Am J Obstet Gynecol* 2009; **200**: 7–9.
21. Chao LW, Chen CH. Spontaneous rupture of an ovarian artery aneurysm: Case report and review of the literature. *Gynecol Obstet Invest* 2009; **68**: 104–107.
22. Barrett JM, Van Hooydonk JE, Boehm FH. Pregnancy-related rupture of arterial aneurysms. *Obstet Gynecol Surv* 1982; **37**: 557–566.
23. Brown BJ, Heaston DK, Poulson AM, Gabert HA, Mineau DE, Miller FJ Jr. Uncontrollable postpartum bleeding: A new approach to hemostasis through angiographic arterial embolization. *Obstet Gynecol* 1979; **54**: 361–365.
24. Deux JF, Bazot M, Le Blanche AF *et al.* Is selective embolization of uterine arteries a safe alternative to hysterectomy in patients with postpartum hemorrhage? *AJR Am J Roentgenol* 2001; **177**: 145–149.
25. Salomon LJ, deTayrac R, Castaigne-Meary V *et al.* Fertility and pregnancy outcome following pelvic arterial embolization for severe post-partum hemorrhage. A cohort study. *Hum Reprod* 2003; **18**: 849–852.
26. Stancato-Pasik A, Mitty HA, Richard HM 3rd, Eshkar N. Obstetric embolotherapy: Effect on menses and pregnancy. *Radiology* 1997; **204**: 791–793.
27. Ornan D, White R, Pollak J, Tal M. Pelvic embolization for intractable postpartum hemorrhage: Long-term follow-up and implications for fertility. *Obstet Gynecol* 2003; **102**: 904–910.
28. Descargues G, Mauger Tinlot F, Clavier E, Lemoine JP, Marpeau L. Menses, fertility and pregnancy after arterial embolization for the control of postpartum hemorrhage. *Hum Reprod* 2004; **19**: 339–343.
29. Hong TM, Tseng HS, Lee RC, Wang JH, Chang CY. Uterine artery embolization: An effective treatment for intractable obstetric haemorrhage. *Clin Radiol* 2004; **59**: 96–101.
30. Hardeman S, Decroisette E, Marin B *et al.* Fertility after embolization of the uterine arteries to treat obstetrical hemorrhage: A review of 53 cases. *Fertil Steril* 2010; **94**: 2574–2579.
31. Ryu RK, Siddiqi A, Omary RA *et al.* Sonography of delayed effects of uterine artery embolization on ovarian arterial perfusion and function. *AJR Am J Roentgenol* 2003; **181**: 89–92.

THE JOURNAL OF
Obstetrics and Gynaecology Research

doi:10.1111/jog.12424 J. Obstet. Gynaecol. Res. Vol. 40, No. 8: 2010–2013, August 2014

Case of concurrent benign metastasizing leiomyoma in the lung and retroperitoneum, with a focus on its etiology

Toshimitsu Tohya[1], Tomotaka Tajima[1], Yuko Takeshita[1], Kiyotaka Ito[2], Kazumi Kuriwaki[3] and Hidetaka Katabuchi[4]

Departments of [1]Obstetrics and Gynecology, [2]Respiratory Medicine and [3]Pathology, Kumamoto Rosai Hospital, and [4]Department of Obstetrics and Gynecology, Faculty of Life Sciences, Kumamoto University, Kumamoto, Japan

Abstract

We report a rare, simultaneous occurrence of benign metastasizing leiomyoma in the lung and retroperitoneum in a 49-year-old woman who had previously undergone myomectomy at 35 years of age and hysterectomy at 45 years of age for multiple recurrences of histologically benign uterine leiomyomas. At 49 years of age, computed tomography-guided biopsy indicated benign metastasizing leiomyomas in the lung. In addition, a retroperitoneal leiomyoma was found that was resected along with both the ovaries via laparotomy. No sign or symptom of recurrence was observed 5 years later. The coexistence of benign metastasizing leiomyoma in the lung and retroperitoneum following surgery for conventional leiomyomas has rarely been reported. Further, the nature and etiology of benign metastasizing leiomyoma are still not well understood. This case is therefore worth reporting, and exploring its etiology is important.

Key words: human, leiomyoma, lung, metastasis, retroperitoneal leiomyoma.

Introduction

Uterine leiomyomas are the most common benign gynecological smooth muscle tumors, and form a single entity. However, some rare forms of leiomyomas have unusual growth, such as benign metastasizing leiomyoma (BML), parasitic leiomyoma, intravenous leiomyomatosis and disseminated peritoneal leiomyomatosis.[1] These rare growth patterns that contain BML originate from a histologically benign uterine leiomyoma. They are characterized by the presence of multiple smooth muscle nodules frequently located in the lung, abdominal cavity, retroperitoneum, muscular tissue, lymph nodes, blood vessels or even the heart.[1–3] The etiology of these tumors remains controversial. Although these lesions have cancer-like properties, they are slow-growing and have a favorable prognosis. However, due to their rarity, information on their histological origin and detailed classification are lacking. As a result, no modern guidelines have been devised for the treatment of BML.

Case Report

A woman had a history of multiple uterine leiomyomas and a subsequent myomectomy at 35 years of age, in addition to a history of total abdominal hysterectomy because of recurrent multiple uterine leiomyomas at 45 years of age. Pathological analysis of the specimen had revealed a uterine smooth muscle tumor without evidence of malignancy. Five years later, at 49 years of age, she was found to have multiple mass lesions in her lungs at a regular checkup. The clinical examination was unremarkable, and the results

Received: November 1 2013.
Accepted: February 17 2014.
Reprint request to: Dr Toshimitsu Tohya, Department of Obstetrics and Gynecology, Kumamoto Rosai Hospital, 1670 Takeharamachi, Yatsushiro, Kumamoto 866-8533, Japan. Email: sanfu-tohya@kumamotoh.rofuku.go.jp

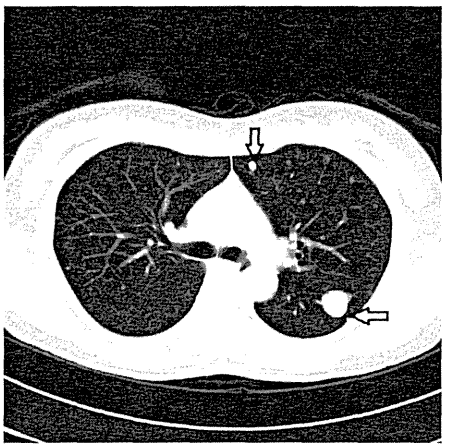

Figure 1 Computed tomography of the chest showing multiple lung lesions. Several nodules are visible in both lungs.

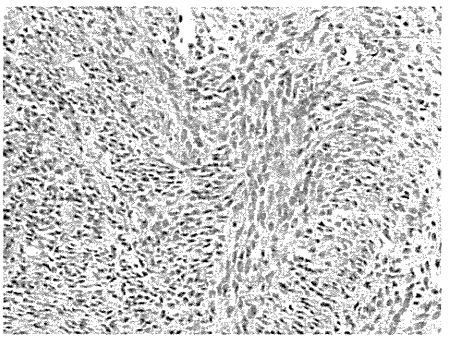

Figure 2 Histological findings of the lung tumors (computed tomography-guided biopsies) (hematoxylin–eosin, original magnification ×400). The tumor contains spindle-shaped smooth muscle cells.

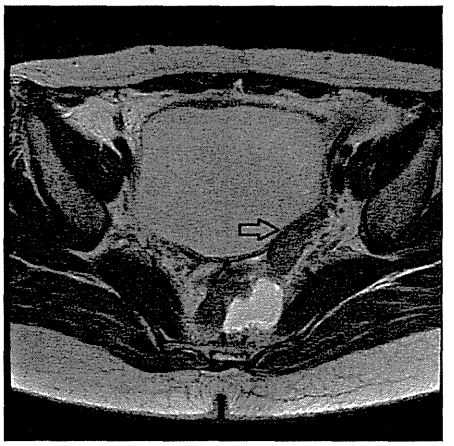

Figure 3 Magnetic resonance image showing a retroperitoneal mass measuring 4 cm × 1.5 cm at the left posterior aspect of the vaginal stump.

from routine laboratory examinations showed normal results. Chest computed tomography (CT) showed multiple solitary nodules in both lungs with maximum diameters of 2 cm (Fig. 1). Positron emission tomography (PET)/CT showed normal ^{18}F-fluorodeoxyglucose uptake and did not indicate the presence of any malignancy. Histological examinations of the samples obtained in the CT-guided biopsy indicated benign leiomyoma. Histopathological examinations of the specimens showed no abnormal mitotic activity. Immunohistochemical examination revealed that the tumor cells were positive for desmin and smooth muscle actin, while they were negative for CD34, c-kit and S-100 (Fig. 2).

In the initial physical and pelvic examination, a firm mass was also detected in the pelvic cavity. Pelvic CT and magnetic resonance imaging showed a retroperitoneal mass measuring 4 cm × 1.5 cm at the left posterior aspect of the vaginal stump in continuity with the vaginal apex (Fig. 3). Tumor markers, including carcinoembryonic antigen, carbohydrate antigen (CA)-19-9 and CA-125 were within the normal ranges. Retroperitoneal mass excision and bilateral salpingo-oophorectomy were performed by laparotomy. On microscopic examination, the retroperitoneal and the lung tumor specimens were not notably different. Based on these findings, we diagnosed these lesions as BML. There has been no sign of recurrence or other symptoms in the following 5 years.

Discussion

Benign metastasizing leiomyoma is a rare cause of pulmonary nodules in middle-aged women with a history

of uterine leiomyoma. Approximately 100 such cases have been reported in the published work,[4] but most of these cases involved pulmonary BML alone. To our knowledge, this is the first case of have been coexistent pulmonary and retroperitoneal BML in Japan.

Benign metastasizing leiomyoma is characterized by a histologically benign smooth muscle tumor originating from a uterine leiomyoma, with the development of similar tumors in distant location. Histological examination of the pulmonary nodules is essential for the diagnosis of BML. In addition, CT-guided biopsies are also now performed. CT examinations of the whole body are important for detecting pulmonary nodules and other lesions associated with this disease. Comparatively, PET examinations have shown negative results in many cases. Before making a diagnosis of BML, leiomyosarcoma or smooth muscle tumors of uncertain malignant potential must be excluded. In most cases, the morphological features and immunohistochemistry should be sufficient for identification, however, the final diagnosis of BML should only be made after a careful review of a substantial number of samples obtained from the primary legion to exclude even small foci of aggressive leiomyosarcoma.[5,6]

There are no established treatments for BML because of the limited number of cases reported. Although the most effective management has not been established, some practical options are present for managing BML. These include careful observation of the clinical course, surgical intervention, and/or chemical castration by removing factors associated with estrogen stimulation by using either bilateral oophorectomy or drugs such as gonadotropin-releasing hormone agonist, progesterone, selective estrogen receptor modulator or aromatase inhibitor.[6] Currently, a class of antiprogestins represents the most specific medical approach to targeting a defined mechanism in leiomyomas.[7] Among these options, careful observation of the clinical course may lead to the best management of BML patients, as they can have a benign indolent clinical course with long-term stability.

The origin and the correct classification of BML remain controversial owing to the obscure nature of the pathogenesis of BML. Several hypotheses have been proposed, one of which speculates that BML is a benign lesion that has the potential for metastasis to the lungs or other organs via a hematogenous route.[8] Considering most BML patients undergo myomectomy or hysterectomy, the occurrence of surgically induced hematogenous propagation of BML cells, which, unlike their more aggressive counterparts, would propagate slowly and be detectable only after several years. A study showed that the mean duration between the hysterectomy and the appearance of the lung lesion was 14.9 years, ranging from 3 months to 20 years.[3] Others have argued that uterine lesions and the associated BML are clonal proliferations, as it is generally recognized that endometriosis can be found at distant sites by the same process.[8] Recently, some interesting studies have reported the etiology of BML. Awonuga *et al.*,[9] who reviewed the published work to outline the possible etiology of BML, found that BML may arise from lymphatic or hematological metastasis, leading to the coelomic metaplasia or intraperitoneal seeding. This evidence that supports the mechanism of the pathogenesis of endometriosis also may be applicable to the pathogenesis of BML.

Other authors[7,10] have reported on the role of stem cells in human uterine leiomyoma growth. Each leiomyoma is a benign monoclonal tumor that arises from a single transformed myometrial smooth muscle cell; however, it is not known which leiomyoma cell type is responsible for tumor growth. These authors hypothesized that a distinct stem/reservoir cell-enriched population, designated as the leiomyoma-derived side population (LMSP), is responsible for cell proliferation and tumor growth, and found that LMSP comprised approximately 1% of all leiomyoma and 2% of all myometrium-derived cells. After resorting and reculturing, LMSP gained full potential for proliferation. Intriguingly, xenografts that comprised LMSP and unsorted myometrial smooth muscle cells grew into relatively large tumors, whereas xenografts that comprised the leiomyoma-derived main population (LMMP) and unsorted myometrial smooth muscle cells produced smaller tumors. LMSP xenografts displayed significantly higher proliferative activity compared with LMMP xenografts ($P < 0.05$). They suggested that LMSP cells, which have stem/reservoir cell characteristics, are necessary for *in vivo* growth of leiomyoma xenograft tumors.

According to the stem cell theory, it can be argued that BML may originate from a stem cell-enriched population of leiomyomas, indicating that despite the complex nature of these disorders, the explanation for their origin may be quite straightforward.

Our case suggests that, in patients with coexistent pulmonary and retroperitoneal BML, from a clinical perspective, we should perform careful follow-up. From a biological perspective, we should analyze the cell population of the associated tumors. Further studies are needed to understand the unique etiology

of this rare disease for the development of better treatment strategies

Disclosure

The authors have no conflict of interest to disclose.

References

1. Zaloudek CJ, Hendrickson MR, Soslow RA. Mesenchymal tumors of the uterus. In: Kurman RJ (ed.). *Blaustein's Pathology of the Female Genital Tract*, 6th edn. New York: Springer-Verlag, 2012; 453–527.
2. Vaquero ME, Magrina JF, Leslie KO. Uterine smooth-muscle tumors with unusual growth patterns. *J Minim Invasive Gynecol* 2009; **16**: 263–268.
3. Moon H, Park SJ, Lee HB *et al*. Pulmonary benign metastasizing leiomyoma in a postmenopausal woman. *Am J Med Sci* 2009; **338**: 72–74.
4. Radzikowska E, Szczepulska-Wojcik E, Langfort R, Oniszh K, Wiatr E. Benign pulmonary metastasizing leiomyoma uteri. Case report and review of literature. *Pneumonol Alergol Pol* 2012; **80**: 560–564.
5. Kayser K, Zink S, Schneider T *et al*. Benign metastasizing leiomyoma of the uterus: Documentation of clinical, immunohistochemical and lectin-histochemical data of ten cases. *Virchows Arch* 2000; **437**: 284–292.
6. Chen S, Zhang Y, Zhang J *et al*. Pulmonary benign metastasizing leiomyoma from uterine leiomyoma. *World J Surg Oncol* 2013; **11**: 163.
7. Bulun SE. Uterine fibroids. *N Engl J Med* 2013; **369**: 1344–1355.
8. Patton KT, Cheng L, Papavero V *et al*. Benign metastasizing leiomyoma: Clonality, telomere length and clinicopathologic analysis. *Mod Pathol* 2006; **19**: 130–140.
9. Awonuga AO, Shavell VI, Imudia AN, Rotas M, Diamond MP, Puscheck EE. Pathogenesis of benign metastasizing leiomyoma: A review. *Obstet Gynecol Surv* 2010; **65**: 189–195.
10. Ono M, Qiang W, Serna VA *et al*. Role of stem cells in human uterine leiomyoma growth. *PLoS ONE* 2012; **7**: e36935.

Int. J. Dev. Biol. 58: 663-668 (2014)
doi: 10.1387/ijdb.140261rn

THE INTERNATIONAL JOURNAL OF DEVELOPMENTAL BIOLOGY
www.intjdevbiol.com

Preformed Wolffian duct regulates Müllerian duct elongation independently of canonical Wnt signaling or Lhx1 expression

MASAHIKO CHIGA[1,2], TOMOKO OHMORI[1], TAKASHI OHBA[2], HIDETAKA KATABUCHI[2] and RYUICHI NISHINAKAMURA*[,1]

[1]*Department of Kidney Development, Institute of Molecular Embryology and Genetics, Kumamoto University and* [2]*Department of Obstetrics and Gynecology, Faculty of Life Sciences, Kumamoto University, Kumamoto, Japan*

ABSTRACT The Müllerian duct gives rise to female reproductive organs, such as the oviduct and uterus. During gestation, the Wolffian duct, which generates male reproductive organs and the kidney, is formed, and the Müllerian duct then elongates caudally along the preformed Wolffian duct. Anatomical separation of these two ducts in chick embryos demonstrated that the Wolffian duct is required for Müllerian duct formation. Likewise, a few reports supported this notion in mice, including studies on *Wnt9b* mutant mice and Wolffian duct-specific *Lhx1* deletion. However, anatomical ablation of the Wolffian duct has not been established in mice. In this study, we addressed the importance of the interaction between these two reproductive ducts, by generating mice that specifically expressed a diphtheria toxin subunit in the Wolffian duct. While this genetic ablation of the Wolffian duct resulted in kidney hypoplasia/agenesis in both male and female mutant mice, the female mutant mice lacked the uterus, which is derived from the Müllerian duct. At mid-gestation, the Müllerian duct was truncated at the level where the mutant Wolffian duct was prematurely terminated, meaning that Müllerian duct elongation was dependent on the preformed Wolffian duct. However, *Wnt9b* expression in the Wolffian duct and the resultant canonical Wnt activity, as well as Lhx1 expression, were not affected in the mutant mice. These results suggest that the Wolffian duct regulates Müllerian duct elongation by currently unidentified mechanisms that are independent of canonical Wnt signaling or Lhx1 expression.

KEY WORDS: *Wolffian duct, Müllerian duct, Wnt9b, Lhx1*

It has been shown that a subset of human patients with uterus hypoplasia display kidney hypoplasia (Oppelt *et al.*, 2007; Woolf and Allen, 1953). While the uterus and the kidney might partially employ similar developmental programs, an interaction between the precursor tissues may also be involved in the formation of these two organs. The reproductive organs in males and females are derived from the Wolffian duct and Müllerian duct, respectively (Kobayashi and Behringer, 2003). The Wolffian duct (mesonephric duct) is first detected at embryonic day (E) 8.5 in mice, and elongates caudally until it reaches the cloaca by E10.5. At E10.5, the ureteric bud stems out from the Wolffian duct, and contributes to the formation of the kidney through a mutual interaction with the metanephric mesenchyme (Nishinakamura, 2008). While most parts of the Wolffian duct degenerate during development, the epididymis and vas deferens in males are derived from the residual Wolffian duct. The Müllerian duct (paramesonephric duct) emerges at E11.5 as an invagination of the peritoneal cavity, and elongates along the preformed Wolffian duct. The Müllerian duct elongation is completed when it reaches the urogenital sinus at E13.5. The Müllerian duct eventually forms the oviduct, uterus, and upper third of the vagina in females, while it starts to degenerate in males between E13 and E14 through the effects of Müllerian inhibiting substance, which belongs to the TGF-β superfamily.

The elongation of the Müllerian duct depends on the preformed Wolffian duct. In chicks, physical elimination of the Wolffian duct or separation of the two ducts using aluminum foil or other methods results in impaired elongation of the Müllerian duct (Bishop-Calame, 1966; Kobayashi and Behringer, 2003). In mice, genetic deletion of genes encoding transcription factors, such as *Pax2*, *Lhx1*, and *Emx2*, results in absence of both the Wolffian duct and Müllerian duct (Miyamoto *et al.*, 1997; Shawlot and Behringer, 1995; Torres *et al.*, 1995). Since these genes are expressed in both ducts, it is difficult to discriminate whether the absence of the Müllerian duct is caused by cell-autonomous requirements of these genes in the

Abbreviations used in this paper: E, embryonic day; md, Müllerian duct; wd, Wolffian duct.

***Address correspondence to:** Ryuichi Nishinakamura. Department of Kidney Development, Institute of Molecular Embryology and Genetics, Kumamoto University, 2-2-1 Honjo, Kumamoto 860-0811, Japan. Tel: +81-96-373-6615. Fax: +81-96-373-6618. E-mail: ryuichi@kumamoto-u.ac.jp

Accepted: 4 December 2014 *by* Makoto Asashima

ISSN: Online 1696-3547, Print 0214-6282

Müllerian duct or by non-cell-autonomous effects caused by loss of the Wolffian duct. Indeed, Müllerian duct-specific *Lhx1* deletion revealed that this gene is required cell-autonomously in the Müllerian duct (Huang *et al.*, 2014). The Müllerian duct tip is considered to contain progenitor-like cells with migratory capacity, which may be responsible for the Müllerian duct elongation. Wolffian duct-specific *Lhx1* deletion impairs not only Wolffian duct formation, but also Müllerian duct elongation (Kobayashi *et al.*, 2005), suggesting that the non-cell-autonomous requirement of the Wolffian duct for Müllerian duct elongation also holds true in mice, although the factors that mediate this Lhx1-dependent process remain unknown.

Wnt9b is expressed in the Wolffian duct and ureteric bud, and evokes the mesenchymal-to-epithelial transition in neighboring tissues (Carroll *et al.*, 2005). *Wnt9b* in the ureteric bud induces the metanephric mesenchyme to form kidney tubules, while that in the Wolffian duct induces the surrounding mesenchyme to form the Müllerian duct. Therefore, deletion of *Wnt9b* affects kidney formation, as well as Müllerian duct elongation. Since the formation of the Wolffian duct is not impaired in *Wnt9b* mutant mice, Wnt9b serves as the only known paracrine molecule to date to explain the non-cell-autonomous effects of the Wolffian duct against Müllerian duct elongation. However, the precise mechanisms of Müllerian duct elongation remain largely unknown. Additionally, physical elimination of the Wolffian duct has not been tested in mice. Therefore, we genetically ablated the Wolffian duct by Wolffian duct-specific expression of a diphtheria toxin subunit, and examined the effects on Müllerian duct elongation.

Results

Hoxb7Cre *is specifically expressed in the Wolffian duct*

Although *Hoxb7Cre* mice are widely used for gene deletion in the Wolffian duct and its derivatives (Yu *et al.*, 2002), we first tried

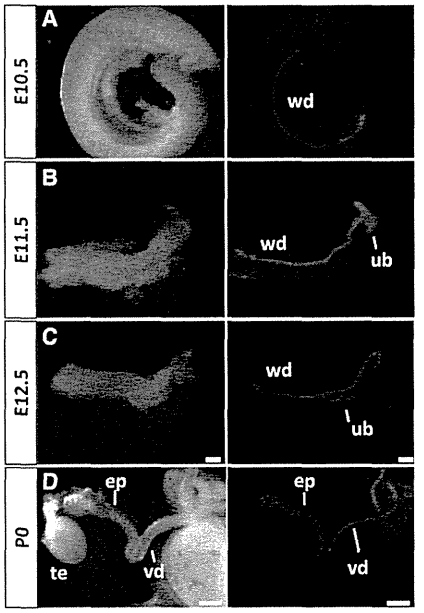

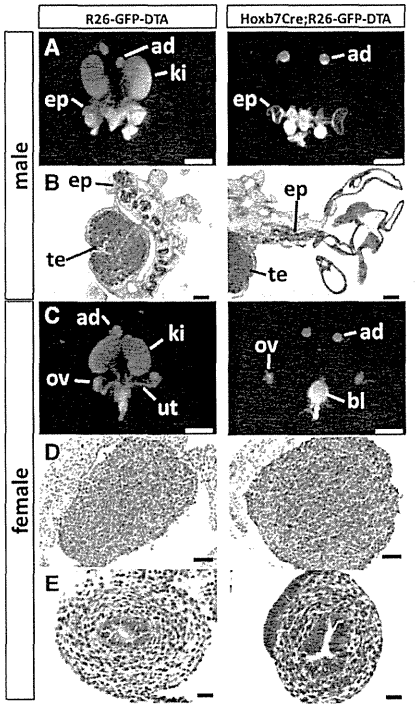

Fig. 1 (left). *Hoxb7Cre* is specifically expressed in the Wolffian duct. *tdTomato expression in* Hoxb7Cre; R26-tdTomato *mice at E10.5, 11.5, 12.5, and P0. Left columns: bright-field images are partly overlaid with tdTomato signals (right columns). ep, epididymis; te, testis; ub, ureteric bud; vd, vas deferens; wd, Wolffian duct. Scale bars (A–C), 200 μm; (D) 500 μm.*

Fig. 2 (right). Wolffian duct ablation causes organ abnormalities derived from both the Wolffian duct and Müllerian duct. (A) *Male urogenital organs in control (*R26-GFP-DTA*) and mutant (*Hoxb7Cre; R26-GFP-DTA*) mice at P0. The kidneys (ki) are absent and the epididymis (ep) is dilated. ad: adrenal gland. Scale bar: 2 mm.* **(B)** *HE-stained frontal sections of the testes (te) and epididymis (ep). Scale bar: 200 μm.* **(C)** *Female urogenital organs in control (*R26-GFP-DTA*) and mutant (*Hoxb7Cre; R26-GFP-DTA*) mice at P0. The kidneys (ki) and uterus (ut) are absent, while the ovaries (ov) and urinary bladder (bl) are retained. Scale bar: 2 μm.* **(D)** *HE-stained frontal sections of the ovaries. Scale bar: 50 μm.* **(E)** *HE-stained frontal sections of the oviducts. Scale bar: 20 μm.*

to eliminate the possibility of ectopic activity, especially in the Müllerian duct. We crossed *Hoxb7Cre* mice with a reporter strain in which the *CAG* promoter, floxed stop sequences, and tandem dimer Tomato (*tdTomato*) coding sequence were inserted into the *Rosa26* locus (Madisen *et al.*, 2010). At E10.5, tdTomato expression was specifically detected in the Wolffian duct (Fig. 1A). tdTomato continued to be expressed in the Wolffian duct, as well as in the kidney-forming ureteric buds, at E11.5 and E12.5 (Fig. 1 B,C), and no ectopic signals were detected. In newborn (P0) males, tdTomato was expressed in the seminiferous tubules, which connect the testis to the excretory route (Fig. 1D). These results reflect the spatially-restricted activity of Cre recombinase in *Hoxb7Cre* mice, in that *Hoxb7Cre* is specifically expressed in the Wolffian duct and its derivatives during development.

Wolffian duct ablation causes organ abnormalities derived from both the Wolffian duct and Müllerian duct

To ablate the Wolffian duct genetically, we crossed *Hoxb7Cre* mice with *R26-GFP-DTA* mice, in which floxed green fluorescent protein (*GFP*) sequences and the diphtheria toxin A subunit (*DTA*) coding sequence were inserted into the *Rosa26* locus (Ivanova *et al.*, 2005). Cre recombinase excises the *GFP* cassette, and activates the downstream *DTA*, thereby efficiently eliminating the Wolffian duct. The resultant newborn mice exhibited hypoplasia or agenesis of the kidneys in all males and females examined (n=4 for each), because the kidney is formed through reciprocal interactions between the metanephric mesenchyme and the Wolffian duct-derived ureteric buds (Fig. 2 A,C). The mutant male mice (four of four) also showed significantly dilated epididymis (Fig. 2B), although the cause of this phenotype remains uninvestigated. Additionally, the mutant female mice (four of four) lacked the uterus, cervix, and upper portion of the vagina, all of which are derived from the Müllerian duct (Fig. 2C). In contrast, the ovary and lower portion of the vagina, which are not derived from the Müllerian duct, developed normally (Fig. 2D and data not shown). Thus, genetic ablation of Wolffian duct-derived tissues caused defects in Müllerian duct-derived organs in female mice. The intact oviducts (Fig. 2E) were likely to result from residual formation of the Müllerian duct, as described for Fig. 3.

Müllerian duct elongation depends on the preformed Wolffian duct

We further examined the elongation of the Wolffian and Müllerian ducts during development. The Wolffian duct in control mice had already elongated and reached the caudal region by E12.5, as shown by *Wnt9b* expression (Fig. 3 A,B, left columns). However, in *Hoxb7Cre; R26-GFP-DTA* mice, the *Wnt9b*-positive Wolffian duct ceased to elongate at the level corresponding to the middle portion of the gonads (Fig. 3 A,B, right columns), indicating successful ablation of the Wolffian duct. This finding is consistent with kidney agenesis observed in newborn mutant mice (Fig. 2 A,C), because the ureteric bud that should be derived from the caudal end of the Wolffian duct is likely to be absent. The residual formation of the Wolffian duct may reflect the possibility that not all of the duct epithelial cells expressed Cre recombinase. Indeed, this transgenic mouse strain uses only a 1.3-kb enhancer/promoter of *Hoxb7* to drive Cre (Yu *et al.*, 2002). It is also noteworthy that *Wnt9b* expression was retained in the residual Wolffian duct.

Next, we used an *Lhx1* probe to visualize the Müllerian duct, and less weakly the Wolffian duct. At E12.5, the Müllerian duct in control mice was in the elongation process, and reached the caudal end by E13.5 (Fig. 3 C,D, left columns). However, elongation of the mutant Müllerian ducts was halted at the same level where the Wolffian ducts were terminated (Fig. 3 C,D, right columns). We did not observe significant differences in this phenotype between male and female embryos (n=12 at E12.5 and n=6 at E13.5), partly because degeneration of the Müllerian duct started between E13 and E14. Thus, Müllerian duct elongation was dependent on the preformed Wolffian duct. Although *Lhx1* in the Wolffian and Müllerian ducts is essential for Müllerian duct elongation (Huang *et al.*, 2014; Kobayashi *et al.*, 2005), the unaltered *Lhx1* expression observed in both ducts of the mutant mice indicates that loss of *Lhx1* expression is not the major cause of the Müllerian duct defects.

Lhx1 expression is not affected in Müllerian duct epithelia

The caudal tip of the elongating Müllerian duct is in physical contact with the Wolffian duct. This tip region contains proliferating progenitors that, at least partly, contribute to duct elongation (Orvis

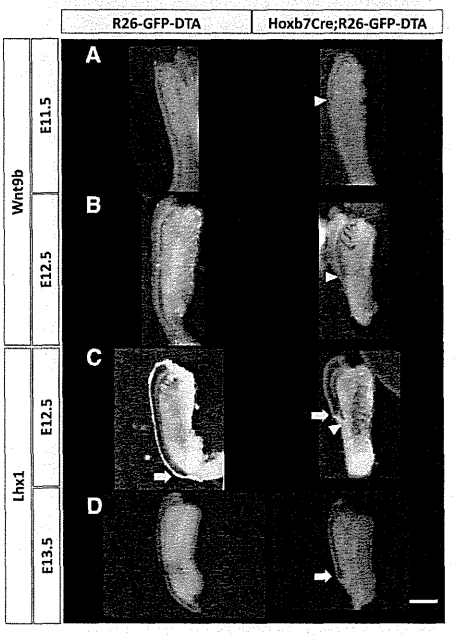

Fig. 3. Müllerian duct elongation depends on the preformed Wolffian duct. (A,B) *Whole-mount* in situ *hybridization of* Wnt9b *at E11.5 and E12.5 in control (*R26-GFP-DTA*) and mutant (*Hoxb7Cre; R26-GFP-DTA*) embryos. The Wolffian ducts are prematurely terminated (arrowheads).* **(C,D)** *Whole-mount* in situ *hybridization of* Lhx1 *at E12.5 and E13.5 in control and mutant embryos. The Müllerian ducts elongate up to the point where the Wolffian ducts are terminated (arrowheads). Arrows: Müllerian duct tips. Scale bar, 200 μm.*

and Behringer, 2007). It is also reported that the tip cells exhibit dynamic morphological changes, forming and retracting multiple cytoplasmic extensions, which suggests a migratory activity of the tip cells (Huang *et al.*, 2014). Thus, we performed histological examinations using sections of the tip region of the elongating Müllerian duct at E12.5. Proliferation of the Müllerian epithelia in the mutant embryos was not significantly impaired, as measured by bromodeoxyuridine (BrdU) incorporation (Fig. 4 A,B). The percentage of BrdU-positive Müllerian duct tips was 27.2±12.6% (455 cells counted) and 16.7±12.3% (262 cells counted) in control and mutant embryos, respectively (n=4 and n=3; p=0.17). Very few apoptotic cells were detected in the Müllerian duct in both control and mutant mice, while some apoptotic cells were detected in the Wolffian duct (Fig. 4C). The percentage of TUNEL-positive cells at the tip of the Müllerian duct was 0.4±0.7% (163 cells counted) and 2.5±3.4% (204 cells counted) in control and mutant mice, respectively (n=3 and n=4; p=0.27). In these experiments, Pax2 was co-stained to identify both the Wolffian and Müllerian ducts. *Pax2* is important for Müllerian duct development (Torres *et al.*, 1995), but its expression was not impaired in mutant embryos (Fig. 4 B,C). Therefore, our data suggest that Müllerian duct truncation may be caused by other mechanisms, possibly including a migration defect of the tip cells. Indeed, we noticed that the tip of

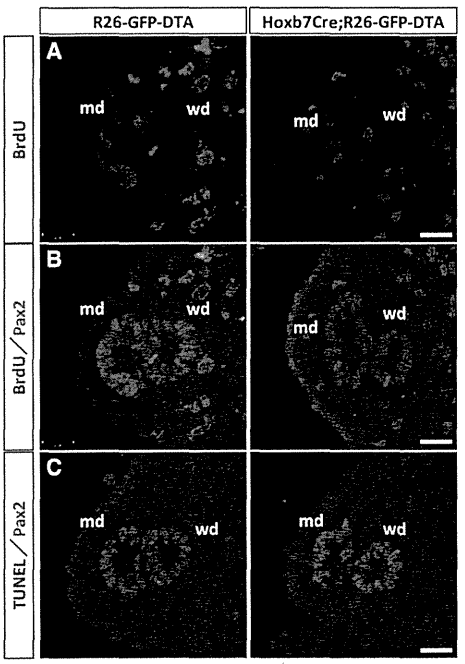

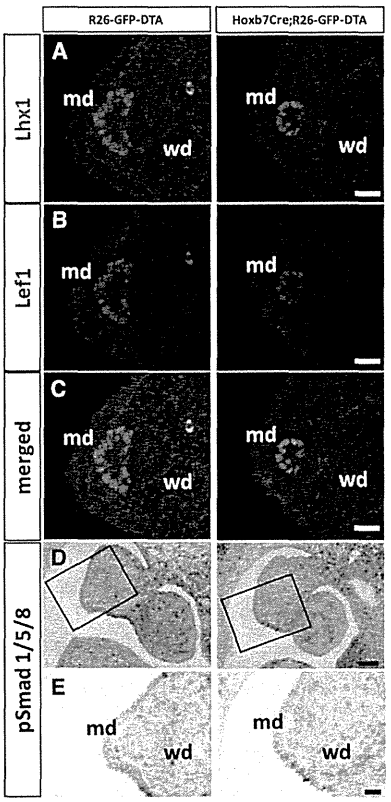

Fig. 4 (left). Proliferation or survival is not affected in Müllerian duct epithelia. (A,B) *BrdU (red) and Pax2 (green) staining in control (*R26-GFP-DTA*) and mutant (*Hoxb7Cre; R26-GFP-DTA*) embryos at E12.5. Significant proliferation defects are not observed in the mutant embryos.* **(C)** *TUNEL (red) and Pax2 (green) staining in control (*R26-GFP-DTA*) and mutant (*Hoxb7Cre; R26-GFP-DTA*) embryos at E12.5. Apoptotic cells are not increased in the mutant Müllerian ducts. md, Müllerian duct; wd, Wolffian duct. Scale bar, 20 μm.*

Fig. 5 (right). Lhx1 expression and canonical Wnt signaling are not affected in the mutant Müllerian tips. (A) *Lhx1 staining (green) in control (*R26-GFP-DTA*) and mutant (*Hoxb7Cre; R26-GFP-DTA*) embryos at E12.5. Lhx1 and Lef1 are co-stained, but each color is presented separately. Although* Lhx1 *is expressed in both Wolffian and Müllerian ducts, the antibody that we used only stained the Müllerian duct, which may reflect the different expression levels of the protein.* **(B)** *Lef1 staining (red) at E12.5. The same sections in (A) were subjected to double-staining. Note that Lef1 staining is detected only in the Müllerian duct epithelia, but not in the Wolffian ducts.* **(C)** *Merged images of Lhx1 and Lef1 staining.* **(D)** *pSmad1/5/8 staining (blue signal) at E12.5. Nuclei were counterstained with Nuclear Fast Red.* **(E)** *Higher magnification of (D). Signals are undetectable in both the control and mutant Müllerian ducts. md, Müllerian duct; wd, Wolffian duct. Scale bars, (A–C, E) 20 μm, (D) 50 μm.*